ELSEVIER

Colloids and Surfaces
A: Physicochemical and Engineering Aspects 152 (1999) 161–182

COLLOIDS AND SURFACES A

Flocculation and coalescence of micron-size emulsion droplets

Ivan B. Ivanov *, Krassimir D. Danov, Peter A. Kralchevsky

Laboratory of Thermodynamics and Physico-chemical Hydrodynamics, Faculty of Chemistry, University of Sofia, Sofia 1126, Bulgaria

Received 11 February 1998; accepted 11 March 1998

Abstract

We analyze the relative importance of droplet deformation, surfactant transfer and interfacial rheology for the properties and stability of emulsions. The appearance of deformation (flattening or film) in the zone of contact of two interacting droplets has the following consequences. It enhances the importance of the surface forces of intermolecular origin and gives rise to contributions from the interfacial dilatation and the bending energy. The flattening increases the viscous dissipation in the gap between two colliding drops and thus prolongs the lifetime of the doublet of two such drops. The critical thickness of the gap also depends on whether the drops are deformed or non-deformed. The factors which facilitate the flattening in the zone of contact between two emulsion drops are the increase in droplet size, the decrease in interfacial tension, the bending energy for water-in-oil emulsions, the increase in droplet–droplet attraction and the suppression of droplet–droplet repulsion. The presence of surfactant strongly affects the interfacial tension, the bending moment, and influences all kinds of DLVO and non-DLVO surface forces operative in the gap between two droplets. The rheological and dynamic properties of the surfactant adsorption monolayers (Gibbs elasticity, surface diffusivity, surface viscosity, and adsorption relaxation time) are major factors for the stability of emulsions under dynamic conditions. The solubility of the surfactant in one of the two phases can determine whether oil-in-water or water-in-oil emulsion will be formed. A criterion for emulsion stability accounting for the interplay of all thermodynamic and hydrodynamic factors mentioned above is obtained. It provides an interpretation and generalization of the Bancroft rule.

Keywords: Bancroft rule; Bending energy of interfaces; Coalescence in emulsions; Emulsion stability; Flocculation in emulsions; Oscillatory structural forces; Surface diffusivity; Surface elasticity; Surface viscosity; Surfactant micelles in emulsions

1. Introduction

The interaction between two colliding emulsion drops of radius a occurs across a narrow gap (thin film) between them. The hydrodynamic forces are due to the viscous friction and can be rather long range. The intermolecular forces of interaction between two drops can have various components: van der Waals, electrostatic, steric, structural, etc. (see Section 2.3). The interplay of these interactions can lead to different results when two drops collide: (i) the drops can rebound; (ii) they can flocculate if the intermolecular repulsive forces are sufficiently strong to hold the drops separated at a small equilibrium distance; (iii) they can coalesce if the film ruptures. We have shown that these processes can occur in a very different manner depending on (1) the drop size and (2) the surfactant properties and distribution.

* Corresponding author. Fax: +359 2 962 56 43.
E-mail address: ivan.ivanov@ltph.bol.bg (I.B. Ivanov)

0927-7757/99/$ – see front matter
PII: S0927-7757(98)00620-7

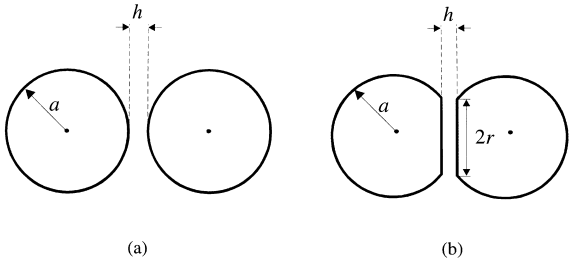

Fig. 1. Sketch of two emulsion droplets of radius a separated at a surface-to-surface distance h. (a) For large h the drops are spherical; (b) for small h a flattening (film) appears in the zone of droplet contact. The film thickness, h, and the film radius, r, are exaggerated in the picture.

(1) If the drops are relatively large, at a given gap width (inversion thickness h_i) the interactions of both hydrodynamic and intermolecular origin deform their caps, which flatten, and an almost planar film forms [1,2], see Fig. 1. On the contrary, small drops keep their shape practically spherical [Fig. 1(a)] up to the moment of flocculation or coalescence. As shown below, the approach of large and small drops and the rupture of the intervening film follow totally different trends, which affect strongly the drop lifetime and its dependence on the parameters of the system.

(2) The surfactant not only influences in many ways the intermolecular interactions across the film, but also creates gradients of the interfacial tension (Marangoni effect). The latter oppose the film drainage and reduce the rate of approach compared with what it would have been in the absence of surfactant. At the same time, the surfactant is usually unable to arrest fully the interfacial motion so that the drops cannot be treated as having "solid" (immobile) interfaces.

The role of the drop size deserves more comment. Depending on their research interests, most scientists consider the drops either as being always spheres (small drops) or concentrate their attention only on the intermolecular and hydrodynamic interactions inside the intervening planar film between large drops, neglecting totally the role of the spherical parts of the drops which are outside the zone of flattening. Our experience shows that in real emulsions the situation is much more complicated, especially for micron-size drops. (i) Depending on various factors, discussed below, drops of the same size can be either spheres or be flattened (truncated spheres) with intervening planar film, i.e. the size is not the only factor governing the drop shape, and thereby its behavior. (ii) Even when there is a planar film, the spherical parts of the drops, outside the planar film, can play a substantial (and sometimes decisive) role for the drop–drop interaction and emulsion behavior. The second effect has been totally ignored in all papers we are aware of. The goal of the present article is to demonstrate the role of the above effects, to reveal and discuss the major factors governing the drop shape and to report some of our recent findings on the interaction, hydrodynamic behavior and lifetime of small deformed and non-deformed drops.

In general, the effects of drop size and surfactant on the flocculation and/or coalescence in emulsions can follow different patterns, which gives rise to a variety of interesting effects. Some of them are briefly considered below; more details can be found in the quoted references.

First of all, let us focus our attention on the effect of the droplet deformability. There is experimental evidence that this effect can substantially influence the droplet–droplet interactions and the overall equilibrium properties of emulsions. Aronson and Princen [3,4] investigated the coexistence of single drops with flocs, the latter being aggregated drops separated by thin liquid films. Hofman and Stein [5] studied experimentally the flocculation of emulsions containing droplets of micrometer size and interpreted some of the results with the droplet deformation at certain conditions (high ionic strength and low interfacial tension). A similar interpretation was proposed for experimental results about the droplet–droplet interactions in microemulsions [6].

The effect of droplet deformation has thermodynamic and hydrodynamic aspects, which are consecutively considered below.

2. Thermodynamic aspects of droplet deformation

2.1. Energy of interaction between two deformable drops

Deformation of a droplet at fixed volume leads to an expansion of the droplet area. In addition,

the flattening of the droplet surfaces in the zone of their contact [Fig. 1(b)] is accompanied by a variation of the interfacial bending energy of the droplets. Last but not least, the formation of a thin liquid film between the two drops greatly enhances the role of surface forces, such as the van der Waals attraction, electrostatic repulsion, hydration, ionic correlation, protrusion and oscillatory structural forces, steric interactions, etc.

In ref. [7] it was demonstrated that the droplet–droplet interaction energy calculated for the model shape of truncated spheres [see Fig. 1(b)] quantitatively agrees very well with the energy calculated by means of the ''real profile'', i.e. by accounting for the gradual transition between the flat film and the spherical portions of the drop surfaces. Therefore, below we will use the configuration of truncated spheres depicted in Fig. 1(b).

In ref. [8] it was shown that the energy of interaction between two deformed emulsion droplets, W, depends on two geometrical parameters, the film thickness, h, and the film radius, r, i.e. $W=W(h, r)$, see Fig. 1(b). On the other hand, it is natural to present the interaction energy as a function of the distance z between the droplet mass centers, i.e. $W=W(z)$. In the rigorous approach to this problem, see ref. [9], the dependence of the interaction energy on the distance z is characterized by the potential of the mean force, $w_f(z)=-kT\ln g(z)$, where k is the Boltzmann constant, T is temperature, and $g(z)$ is the pair (radial) correlation function. The latter function is determined by statistical averaging over all possible droplet configurations (of various h and r) corresponding to a given z:

$$g(z)=1.103\left(\frac{\pi a^2\sigma}{2kT}\right)^{1/4}\frac{1}{a}\int\exp\{-W[h(r), r]/kT\}\,\mathrm{d}r \tag{1}$$

Here a and σ are the drop radius and the interfacial tension; $h(r)$ represents the geometrical relation between h and r for fixed z and drop volume. To calculate $w_f(z)$ one needs to know the function $W=W(h, r)$, which may contain contributions due to various effects considered below.

2.2. Contribution of the interfacial deformation to $W(h, r)$

2.2.1. Effect of the interfacial dilatation

It is assumed that, before the collision, the two droplets are spheres of radius a [Fig. 1(a)]. When the distance between the droplets is small enough, a flattening [film of radius r, Fig. 1(b)] could appear in the zone of their contact. This deviation from the spherical shape causes a dilatation of the droplet surface; the respective increase of the surface energy of the two drops follows from simple geometrical considerations [6,8,9]:

$$W_{\mathrm{dil}}=\sigma\frac{\pi r^4}{2a^2}+\frac{1}{2}E_{\mathrm{G}}\left(\frac{\pi r^4}{2a^2}\right)^2+\ldots,\quad \text{for } \left(\frac{r}{a}\right)^2\ll 1 \tag{2}$$

Our calculations show that for typical emulsion systems the condition $(r/a)^2\ll 1$ is always satisfied and Eq. (2) holds with good precision. Most often, W_{dil} is determined by the change of area [this is accounted for by the first term in Eq. (2), proportional to the interfacial tension σ]. The contribution of the surface (Gibbs) elasticity, E_{G} (due to the change of σ) to W_{dil} is usually a higher order effect and can be neglected. However, for microemulsions $\sigma\ll 1$ mN/m and the term with E_{G} in Eq. (2) may become predominant. In all cases Eq. (2) predicts that W_{dil} strongly increases with film radius r, i.e. with deformation. Note that $W_{\mathrm{dil}}>0$, i.e. the interfacial dilatation gives rise to an effective repulsion between the two droplets.

2.2.2. Effect of interfacial bending

The flattening of the drop surfaces in the zone of contact [Fig. 1(b)] is affected by the interfacial bending moment, B_0. Hence, work of interfacial flexural deformation must be performed to achieve deformation [2]:

$$W_{\mathrm{bend}}=-2\pi r^2B_0/a,\quad (r/a)^2\ll 1 \tag{3}$$

Note that $B_0=-4k_{\mathrm{c}}H_0$, where H_0 is the so-called spontaneous curvature and k_{c} is the interfacial curvature elastic modulus; typically B_0 is of the order of 5×10^{-11} N (see ref. [10] for details). For oil-in-water (O/W) emulsions B_0 usually opposes the flattening of the droplet surfaces in the zone

of collision, but for water-in-oil (W/O) emulsions B_0 favors the flattening [2]. Therefore, $W_{\text{bend}}>0$ for two droplets in an O/W emulsion, while $W_{\text{bend}}<0$ for a couple of droplets in a W/O emulsion. Since it is easier for two drops to coalesce when a planar film already exists between them, one can conclude that the interfacial bending moment stabilizes the O/W emulsions, but destabilizes the W/O ones. There is experimental evidence [11] for droplet aggregation in W/O microemulsions, which can be attributed (at least in part) to the effect of W_{bend}. It is interesting to note that the effect of the bending moment can be important even for droplets of micrometer size [2]. Indeed, assuming $a=1$ μm, $r\approx a/50$, $|B_0|=5\times 10^{-11}$ N (see e.g. ref. [10]), from Eq. (3) one calculates $|W_{\text{bend}}|\approx 31kT$.

By means of similar considerations one can deduce [2] that an emulsion containing microemulsion droplets in the continuous phase should be more stable than an emulsion containing microemulsion droplets in the disperse phase, as was observed experimentally [12,13].

2.3. Contribution of the surface forces to $W(h, r)$

2.3.1. Van der Waals interaction

Based on the assumption for pairwise additivity of the van der Waals interaction energy with respect to the couples of molecules, one may derive (see ref. [8]) an exact (though rather long) expression for the energy, W_{vw}, of the van der Waals interactions between two deformed drops of equal size [Fig. 1(b)]. In most cases an approximate expression (for moderate deformations and separations) holds with very good precision [2,9]:

$$W_{\text{vw}}(h, r)=-\frac{A_{\text{H}}}{12}\left[\frac{3}{4}+\frac{a}{h}+2\ln\left(\frac{h}{a}\right)+\frac{r^2}{h^2}-\frac{2r^2}{ah}\right], \quad \text{for } \frac{h}{a}<0.3, \frac{r}{a}<0.5 \tag{4}$$

where A_{H} is the Hamaker constant. More general expressions for arbitrarily deformed spheres of different size (as well as for a deformable sphere and a wall) are given in ref. [8].

2.3.2. Electrostatic interaction

The rigorous theory of the electrostatic (double layer) interaction yields rather complicated expressions for the respective interaction energy, even in the simpler case of a plane-parallel liquid film [14,15]. Fortunately, some useful approximate expressions could be derived. By using the Derjaguin approximation [15], one can obtain [8]:

$$W(h, r)=\pi r^2 f(h)+\pi a\int_h^\infty f(H)\,\mathrm{d}H \tag{5}$$

Here W is the energy of interaction of the two droplets, $f(h)$ is the interaction energy per unit area in a plane-parallel film; the first term on the right-hand side of Eq. (5) expresses the interaction across the flat film of radius r, whereas the last term in Eq. (5) accounts for the interaction across the Plateau border encircling the flat film [Fig. 1(b)]. Note that by definition:

$$f(h)=\int_h^\infty \Pi(H)\,\mathrm{d}H \tag{6}$$

where $\Pi(H)$ is the disjoining pressure of a plane-parallel film of thickness H [15].

Eq. (5) can be applied to any type of surface force (irrespective of its physical origin) if only the range of action of this force is much smaller than the drop radius a. In the special case of electrostatic interaction and weak double layer overlap, the substitution of the Verwey–Overbeek [14] expression for $f_{\text{el}}(H)$ in Eq. (5) yields [7–9]:

$$W_{\text{el}}(h, r)=\frac{64\pi C_{\text{el}}kT}{\kappa}\tanh^2\left(\frac{Ze\psi_0}{4kT}\right)\times\exp(-\kappa h)\left[r^2+\frac{a}{\kappa}\right]; \quad \kappa^2=\frac{2Z^2e^2}{\epsilon_0\epsilon kT}C_{\text{el}} \tag{7}$$

where κ^{-1} is the Debye screening length, C_{el} (cm^{-3}) is the concentration of a symmetric Z:Z electrolyte, ϵ denotes the dielectric permittivity; ψ_0 is the surface potential of the droplet.

Fig. 2(a) shows a contour plot of $W(h, r)\equiv W_{\text{dil}}+W_{\text{vw}}+W_{\text{el}}$ for $a=1$ μm, $\psi_0=100$ mV, $\sigma=1$ mN/m, $C_{\text{el}}=0.1$ M, $A_{\text{H}}=2\times 10^{-20}$ J. The minimum of the potential surface, corresponding to an

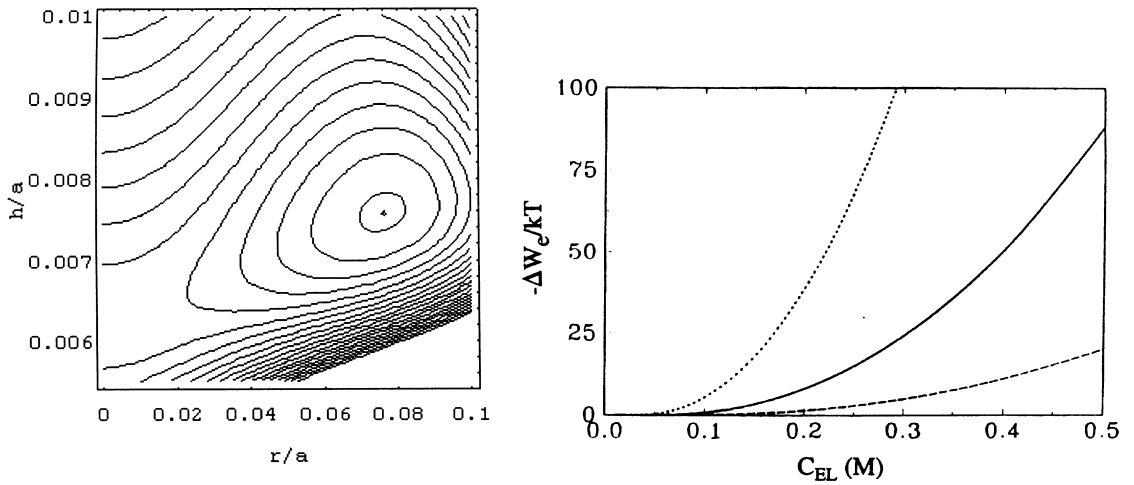

Fig. 2. (a) Contour plot of the total drop–drop interaction energy, $W(h, r)=W_{dil}+W_{vw}+W_{el}$ for various values of h/a and r/a, see Fig. 1 for notation. The values of the parameters are as follows: $a=1$ μm, $\psi_0=100$ mV, $\sigma=1$ mN/m, $C_{el}=0.1$ M, $A_H=2\times10^{-20}$ J. The distance between two contours equals $2kT$; the minimum of the potential surface is $W(h_e, r_e)=-60kT$. (b) Plot of $\Delta W_e\equiv W(h_e, r_e)=W(h^*, 0)$ vs. electrolyte concentration C_{el} for $A_H=1\times10^{-20}$ J and three values of the drop radius: $a=0.5$, 1.0 and 2.0 μm for the dashed, continuous and dotted lines, respectively.

equilibrium doublet of drops, has a depth $W(h_e, r_e)=-60kT$. Hence, the equilibrium doublet should be rather stable. As shown in ref. [2], the radius of the equilibrium doublet, r_e, increases with the rise of both C_{el} and the drop radius a. Let us denote by $W(h^*, 0)$ the minimum value of W along the ordinate axis in Fig. 2(a), corresponding to two spherical (non-deformed) drops, see Fig. 1(a). Fig. 2(b) shows $\Delta W_e\equiv W(h_e, r_e)-W(h^*, 0)$ vs. C_{el} for three values of the drop radius a. One sees that the effect of droplet deformation, expressed by ΔW_e, strongly increases with the rise of C_{el} and a.

The double layer and van der Waals interactions are often termed "DLVO surface forces", since they were involved in the first version of the theory of colloid stability [14,15]. Other surface forces, found later, are called "non-DLVO" surface forces [16]. The contributions of some of these forces to $W(h, r)$ are briefly considered below.

2.3.3. Ionic correlation surface force

As shown by Debye and Hückel, the energy of formation of the counterion atmospheres of the ions in a solution gives a contribution to the free energy of the solution called "correlation energy". This correlation energy provides a contribution to the osmotic pressure of an electrolyte solution. Since the electrostatic disjoining pressure is actually an excess osmotic pressure in the thin liquid film [14–16], it must include also a contribution from the correlation energy, which is not taken into account in the conventional DLVO theory. Both numerical and analytical methods have been developed for calculating the contribution of the ionic correlations, f_{cor}, to the interaction free energy $f(h)$ — for a review see ref. [17]. Combining Eq. (5) with the asymptotic formula derived by Attard et al. [18], one obtains an expression for the contribution of the ionic correlations to the droplet–droplet interaction energy $W(h, r)$ for the case when the electrolyte is symmetrical (Z:Z) and $\exp(-\kappa h)\ll1$:

$$W_{cor}=W_{el}\frac{Z^2e^2\kappa}{16\pi\epsilon\epsilon_0kT}(\ln 2+2I_C) \quad (8)$$

where W_{el} is the conventional DLVO electrostatic

energy, Eq. (7):

$$I_C = \frac{2-2z^3+z}{2z(2z^2-1)^2} - \frac{1}{2}(1-J)\ln(z+z^2) - \frac{\sqrt{z^2-1}}{z}[1+J+4(2z^2-1)^{-3}]\arctan\sqrt{\frac{z-1}{z+1}} + \frac{1}{2}(1+J)\ln 2; \quad J \equiv \frac{2z^2-3}{(2z^2-1)^3},$$

$$z \equiv \left[1+\left(\frac{e\sigma_s}{2\epsilon\epsilon_0 kT\kappa}\right)^2\right]^{1/2}$$

and σ_s is the surface charge density. As a rule, W_{cor} is negative and corresponds to attraction; its magnitude increases with the rise of C_{el} and σ_s. In the case of 1:1 electrolyte, W_{cor} is usually small compared with W_{el}. In the case of 2:2 electrolyte, however, the situation can be quite different: the attractive forces, $W_{cor}+W_{vw}$, can prevail over W_{el} and the total energy, W, can become negative virtually on the entire thickness range. In the presence of bivalent and multivalent counterions, W_{cor} can become the dominant surface force and should necessarily be taken into account, see e.g. ref. [19].

2.3.4. Hydration repulsion

The hydration repulsion is a short-range monotonic repulsive force which appears as a deviation from the DLVO theory for short distances between two molecularly smooth electrically charged surfaces [16]. Such a force may appear in foam or emulsion films stabilized by ionic surfactants. The physical importance of the hydration force is that it stabilizes the thin films (and thereby the emulsions), thus preventing coagulation in the primary minimum of the DLVO disjoining pressure isotherm [14–16]. It is believed that the hydration force is connected with the binding of strongly hydrated ions (such as Mg^{2+}, Li^+, Na^+) to the interface. Empirically, this force, called the hydration repulsion, follows an exponential law [16]. The substitution of this exponential law in Eq. (5) yields an expression for estimating the contribution of the hydration repulsion to the droplet–droplet interaction energy, $W(h, r)$:

$$W_{hydr}(h, r) = \pi f_0 \exp(-h/\lambda_0)[r^2 + a\lambda_0] \quad (9)$$

where, as usual, h is the film thickness; the decay length $\lambda_0 \approx 0.6$–1.1 nm for 1:1 electrolytes; the pre-exponential factor, f_0, depends on the hydration of the surfaces but is usually about 3–30 mJ/m^2 [16]. It seems that the main contribution to the hydration repulsion between two charged interfaces originates from the finite size of the hydrated counterions [20], an effect which is not taken into account in the DLVO theory (the latter deals with point ions). For more accurate calculation of W_{hydr} we recommend the theory from ref. [20] be used.

2.3.5. Protrusion and steric interaction

Due to its thermal motion, an amphiphilic molecule in an adsorption monolayer (or micelle) may fluctuate around its equilibrium position, i.e. may protrude. The configurational confinement of the protruding molecules within the narrow space between two approaching interfaces gives rise to a short-range repulsive surface force, called the protrusion force [21]. The effect can be important for the stability of very thin emulsion films. The energy of molecular protrusion can be presented in the form $u(x) = \alpha x$, where x is the distance out of the oil–water interface ($x > 0$) with $\alpha = 3 \times 10^{-11}$ J/m for single-chained surfactants [21,22]. By using a mean-field approach, Israelachvili and Wennerström [21] derived an expression for the protrusion disjoining pressure which can be combined with our Eq. (5) to yield:

$$W_{protr}(h, r) \approx -\pi r^2 \Gamma kT \ln[1-(1+h/\lambda)\exp(-h/\lambda)], \quad \lambda \equiv \frac{kT}{\alpha} \quad (10)$$

λ has the meaning of protrusion decay length; $\lambda =$ 0.14 nm at 25°C; Γ denotes the number of protrusion sites per unit area. Note that W_{protr} decays exponentially for $h \gg \lambda$, but $W_{protr} \propto -\ln(h/\lambda)$ for $h < \lambda$, i.e. W_{protr} is divergent for $h \to 0$.

In fact, the protrusion force is a kind of steric interaction due to the overlap of spatially "diffuse" and thermally mobile interfacial zones. In the case

of adsorption monolayers of non-ionic surfactants, the steric repulsion originates from the overlap of the "brushes" of polyoxyethylene chains at the surfaces of two approaching emulsion droplets. Expressions appropriate for calculating $W(h, r)$ in this case can be found in ref. [2].

2.3.6. Oscillatory structural force

Very often, the emulsions contain small colloidal particles (such as surfactant micelles or protein globules) in the continuous phase. The presence of these small particles gives rise to the oscillatory structural force, which affects the stability of foam and emulsion films as well as the flocculation processes in various colloids [23]. At higher particle concentrations (volume fractions above 15%), the structural forces stabilize the liquid films and emulsions. At lower particle concentrations the structural forces degenerate into the so-called depletion attraction, which is found to destabilize the dispersions [16]. To quantify the contribution of the oscillatory forces, W_{osc}, to $W(h, r)$, one can combine Eq. (5) with the following semi-empirical formula for the oscillatory structural component of disjoining pressure [24]:

$$f_{osc} = \int_h^\infty \Pi_{osc}\, dh;\ \Pi_{osc}(h) = \begin{cases} P_0 \cos\left(\frac{2\pi h}{d_1}\right) \exp\left(\frac{d^3}{d_1^2 d_2} - \frac{h}{d_2}\right) & \text{for } h > d \\ -P_0 & \text{for } 0 < h < d \end{cases} \quad (11)$$

Here d is the diameter of the small particles (micelles), d_1 and d_2 are the period and the decay length of the oscillations; P_0 is the particle osmotic pressure in the bulk solution. P_0, d_1 and d_2 do not depend on h, but depend on the particle (micelle) volume fraction, φ; the respective expressions can be found in refs. [17,24–26]. The contour plot of $W_{osc}(h, r)$, similar to Fig. 2(a), exhibits several local minima separated by "mountain ranges" —

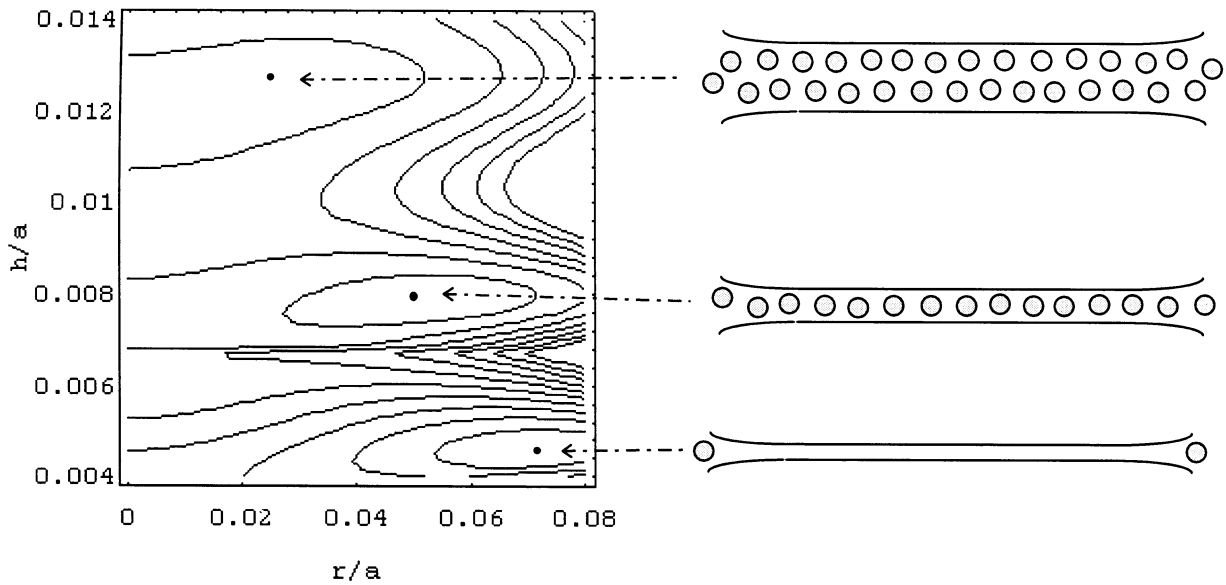

Fig. 3. Contour plot of the energy, $W(h, r) = W_{dil} + W_{vw} + W_{el} + W_{osc}$ between two oil drops of radius $a = 2$ μm in the presence of ionic micelles in water. The parameters correspond to a micellar solution of sodium nonylphenol polyoxyethylene-25 (SNP-25S): $d =$ 9.8 nm, $\varphi = 0.38$, $\sigma = 7.5$ mN/m, $A_H = 5 \times 10^{-21}$ J, $\psi_0 = -135$ mV, $C_{el} = 25$ mM, $\kappa^{-1} = 1.91$ nm [25,26]. The points on the contour plot correspond to three local minima: $W/kT = 406$, -140, and -37, corresponding to films containing zero, one and two micellar layers, respectively.

see Fig. 3. When the particle volume fraction is smaller than ca. 10% in the continuous phase, the height of the taller "range" is smaller than kT, and it cannot prevent the flocculation of two droplets in the deep "depletion" minimum. However, at higher micellar volume fraction these "ranges" act like barriers (Fig. 3) against the closer approach and flocculation (or coalescence) of the droplets in emulsions [2]. An illustration is given in Fig. 4.

The three curves in Fig. 4 correspond to three emulsions containing different concentrations of sodium nonylphenol polyoxyethylene-25 sulfate (SNP25S) in the aqueous phase: 22.3, 33.5 and 67 mM, all of them much above (from 80 up to 240 times) the critical micellization concentration, CMC = 0.28 mM. The height of the column of the aqueous phase, below the emulsion cream, is plotted in Fig. 4 as a function of time. The initial slope of the curves point to the diminishing rate of water separation as the surfactant concentration rises. Moreover, the concentrated system finally produces loosely packed cream (note the positions of the plateaus), possibly due to hampered flocculation. One can attribute the observed effects to the oscillatory structural forces, see refs. [25,26] for details.

2.3.7. Conclusions

In the first part of this paper we demonstrate that even very small emulsion droplets behave as deformable particles and a thin film might be formed between them [Fig. 1(b)]. Many effects can contribute to the energy of interaction between two deformable emulsion droplets, which can be presented in the form:

$$W = W_{\mathrm{dil}} + W_{\mathrm{bend}} + W_{\mathrm{vw}} + W_{\mathrm{el}} + W_{\mathrm{cor}} + W_{\mathrm{hydr}} + W_{\mathrm{protr}} + W_{\mathrm{osc}} + \ldots \quad (12)$$

where the various contributions can be calculated from Eqs. (2)–(11). For each specified system an estimate may reveal which of the terms in Eq. (12) are predominant, and which of them can be neglected. The analysis shows that the same approach can be applied to describe the multidroplet interactions in flocs, because in most cases the interaction energy is pairwise additive.

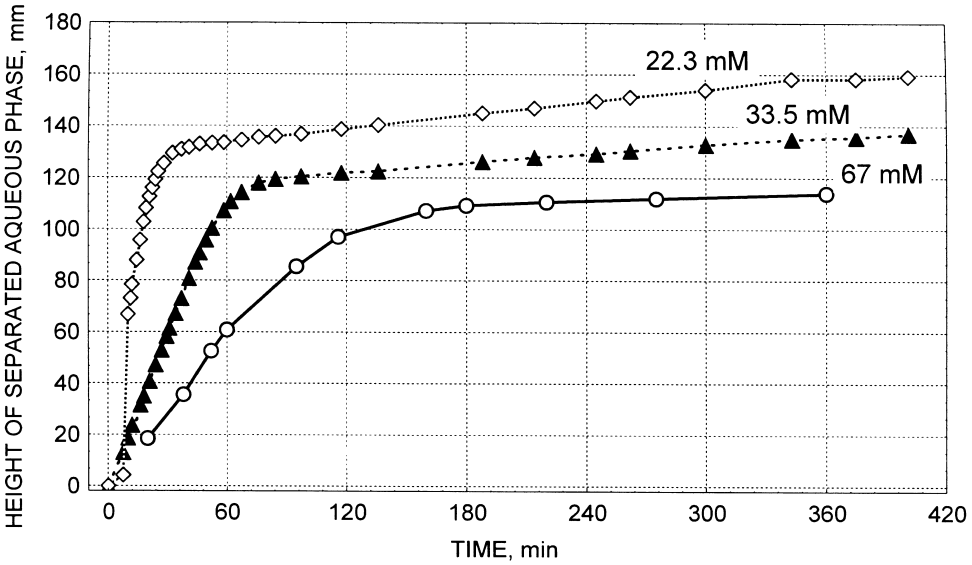

Fig. 4. Plot of the height of the water column, separated below a 20% styrene-in-water emulsion, as a function of time. The curves correspond to different surfactant (SNP-25S) concentrations, denoted in the figure, all of them above the CMC.

3. Hydrodynamic interactions: droplets of tangentially immobile surfaces

In the previous section we showed that two emulsion drops can deform upon collision [Fig. 1(b)] when the droplet–droplet attraction is strong enough, i.e. the depth of the minima in Figs. 2 and 3 is larger than kT. This conclusion is correct, but it is strictly valid only for very slow, quasi-static, approach of two droplets. In reality the viscous dissipation of energy in the zone of droplet collision can also lead to interaction between two emulsion drops and can cause their deformation, see e.g. ref. [27]. This hydrodynamic interaction is considered below.

3.1. Regimes of approach of two droplets

In this section we consider the case of large surfactant concentration in the continuous phase, when the interfacial mobility is completely suppressed by the adsorbed surfactant but the surfaces are still deformable in normal direction, i.e. they are flexible. At comparatively large separations such droplets, moving under the action of a driving force F, will not interact and will obey the Stokes equation for solid spheres, so that their velocity will be:

$$V_{St} = \frac{F}{6\pi\eta a} \tag{13}$$

where η is the dynamic viscosity of the continuous medium, and as usual a denotes the radius of the droplet.

At closer distances the hydrodynamic interaction becomes significant but the drop may still remain spherical [see Fig. 1(a)]. Then, instead of Eq. (13), one must use the Taylor formula [28] for the velocity of approach of two non-deformed spherical droplets:

$$V_{Ta} = \frac{2hF}{3\pi\eta a^2} = V_{St}\frac{4h}{a} \tag{14}$$

Since $h/a \ll 1$, the approach of the two drops is slowed down.

With further approach, when the so-called inversion thickness h_i is reached, the interfacial shape in the gap changes from convex to concave. From a physical viewpoint this is the beginning of the deformation of the droplets in the zone of their contact with subsequent formation of a thin film between them [see Fig. 1(b)]. One can estimate the inversion thickness from the simple expression [29–31]:

$$h_i = F/(2\pi\sigma) \tag{15}$$

where σ is the interfacial tension. Eq. (15) is valid for relatively large surface-to-surface distances between the two drops, when the surface forces (of intermolecular origin) can be neglected. A generalization of Eq. (15), taking into account the contribution of the surface forces, was recently reported in ref. [32]:

$$h_i = \frac{F}{2\pi\bar{\sigma}} + \frac{\bar{a}}{2\bar{\sigma}}\left[h_i \Pi(h_i) - f(h_i)\right] \tag{16}$$

where $\Pi(h)$ and $f(h)$ are the same as in Eq. (6) above. In general, Eq. (16) holds for two dissimilar droplets of radii a_1 and a_2, and surface tensions σ_1 and σ_2; $\bar{a}$ and $\bar{\sigma}$ in Eq. (16) have the meaning of average diameter and surface tension defined as follows:

$$\bar{a} = \frac{2a_1a_2}{a_1+a_2};\ \bar{\sigma} = \frac{2\sigma_1\sigma_2}{\sigma_1+\sigma_2} \tag{17}$$

Generalization of Eq. (16) to the case of drops with tangentially mobile surfaces, for which the Marangoni effect becomes operative, could be found below, see Eq. (38).

After a film is formed in the zone of droplet–droplet contact, the viscous dissipation of energy takes place mostly in this film. Then the rate of approach obeys the Reynolds formula [33], describing the thinning rate of a planar film between two solid discs:

$$V_{Re} = \frac{2h^3}{3\pi\eta r^4}(F - F_W),\ F_W \equiv -\frac{dW}{dh} \tag{18}$$

where h is the distance between the discs (the film thickness), r is the disc (film) radius; F is the external driving force, whereas F_W is the force resulting from the droplet–droplet interaction with

W being the interaction energy defined by Eq. (12) above.

The film radius can be estimated from the balance of the driving and capillary force [29,30]:

$$r^2 \approx \frac{F\bar{a}}{2\pi\bar{\sigma}} \tag{19}$$

For relatively thick films ($F_W \ll F$) we combine Eqs. (18) and (19) to derive:

$$V_{\mathrm{Re}} = \frac{8\pi\bar{\sigma}^2 h^3}{3\eta\bar{a}^2 F} \tag{20}$$

It is interesting to note that in the Reynolds regime [i.e. when there is flattening and Eq. (20) holds], the velocity V_{Re} decreases with the rise of the external driving force F. This tendency is exactly the opposite to that for the particle motion in Stokes or Taylor regimes, cf. Eqs. (13) and (14). A manifestation of this fact is the non-monotonic dependence of the droplet lifetime, τ, on the drop radius, a, which is considered below (see Section 3.2.3).

3.2. Lifetime of emulsion films; critical thickness

3.2.1. Combined expression for the Taylor and Reynolds regimes

It is possible to unify the treatment for the Taylor and Reynolds regimes, Eqs. (14) and (18). The following generalized expression was obtained in ref. [1], eq. (3.19) therein:

$$F = \frac{3}{2}\pi\eta V\frac{\bar{a}^2}{h}\left(1 + \frac{r^2}{h\bar{a}} + \frac{r^4}{h^2\bar{a}^2}\right) \quad (F_W \ll F) \tag{21}$$

where $\bar{a}$ is the average drop radius in the case of two dissimilar drops, see Eq. (17). One sees that for small film radii, $r \to 0$, Eq. (21) reduces to the Taylor Eq. (14), whereas for large films, $r/(h\bar{a}) \gg 1$, Eq. (21) yields the Reynolds Eq. (18). Indeed, expressing the velocity from Eq. (21) one obtains:

$$\frac{1}{V} = \frac{1}{V_{\mathrm{Ta}}} + \frac{1}{\sqrt{V_{\mathrm{Ta}}V_{\mathrm{Re}}}} + \frac{1}{V_{\mathrm{Re}}} \tag{21'}$$

In the case of two emulsion drops moving toward each other under the action of a constant force F with velocity $V = -\mathrm{d}h/\mathrm{d}t$, Eq. (21) can be integrated to obtain an expression for the film lifetime [17]:

$$\tau = \int_{h_c}^{h_{\mathrm{in}}} \frac{\mathrm{d}h}{V} = \frac{3\pi\eta\bar{a}^2}{2F}\left[\ln\frac{h_{\mathrm{in}}}{h_c} + \frac{r^2}{h_c\bar{a}}\left(1 - \frac{h_c}{h_{\mathrm{in}}}\right) + \frac{r^4}{2h_c^2\bar{a}^2}\left(1 - \frac{h_c^2}{h_{\mathrm{in}}^2}\right)\right] \quad (F_W \ll F) \tag{22}$$

h_c denotes the critical thickness of film rupture, and h_{in} is the initial thickness of the film.

In the case of coalescence of a droplet with its homophase (flat oil–water interface), one has $\bar{a} = 2a$, where a is the droplet radius. Then, combining Eqs. (19) and (22) and the expression for the buoyancy force:

$$F = \frac{4}{3}\pi a^3 g\Delta\rho \tag{23}$$

with g and $\Delta\rho$ being the acceleration due to gravity and the density difference, one can calculate $\tau = \tau(a)$ if an expression for the critical thickness, h_c, is available. The physical meaning of h_c is discussed in the next subsection.

3.2.2. Critical thickness of the gap between two spherical drops

The surface of an emulsion droplet is corrugated by capillary waves caused by thermal fluctuations or other perturbations. The surface shape can be represented mathematically as a superposition of Fourier components with different wavenumbers and amplitudes. If attractive disjoining pressure is present, it enhances the amplitude of the corrugations in the zone of contact of the droplets. For every Fourier component there is a film thickness, called the transitional thickness, h_t, at which the respective surface fluctuation becomes unstable and this surface corrugation begins to grow spontaneously [30,31]. At a given film thickness, h_c, called critical, the unstable maximum surface corrugations on the two opposite droplet surfaces can touch each other. We will assume that there are no forces strong enough to hold the two surfaces apart; consequently, the film breaks and the droplets coalescence. We will assume further that the shape at this moment is determined predominantly

by a single Fourier component (critical wave) with wavenumber k_c. It was recently established that in most cases the transitional thickness $h_t(k_c)$ of the critical wave and the film critical thickness h_c are very close, i.e. $h_t(k_c) \approx h_c$, see fig. 44 in ref. [34]. For that reason, below we will disregard the difference between critical and transitional thickness.

An analytical formula for determining the critical thickness h_c (actually the minimum width h) of the gap between two colliding spherical droplets [see Fig. 1(a)] was derived in ref. [32]; h_c is determined as the solution of the following transcendental equation:

$$F - \bar{a}\pi f(h_c) = \frac{\pi \bar{a}^2 h_c^3}{32\bar{\sigma}} \left[\left(\frac{\partial \Pi}{\partial h} \right)_c^2 - \frac{8\bar{\sigma}}{\bar{a}} \left(\frac{\partial^2 \Pi}{\partial h^2} \right)_c \right] \tag{24}$$

where in the left-hand side F is the external driving force and the second term is the interaction force, F_W, see Eq. (5). The subscript "c" in the parentheses means that the respective derivatives must be estimated at $h = h_c$. One can determine h_c by solving numerically Eq. (24). Recall that Eq. (24) holds only for spherical drops, which are practically nondeformed. (Expressions for the critical thickness of a large plane-parallel film were derived long ago, see e.g. refs. [27,30,35] for a discussion.) Generalization of Eq. (24) to the case of drops with tangentially mobile surfaces, for which the Marangoni effect becomes operative, could be found below, see Eq. (39).

The rupture of the film is usually caused by the van der Waals forces which can be calculated from the expression:

$$\Pi(h) = -A_H/(6\pi h^3) \tag{25}$$

with A_H being the Hamaker constant. Using Eqs. (6) and (25) one obtains the following asymptotic forms of Eq. (24):

$$h_c = [\bar{a}^2 A_H^2/(128\pi\bar{\sigma}F)]^{1/5}, \quad \text{for } F \gg \pi\bar{a}f(h_c) \tag{26}$$

$$h_c = [5\bar{a}A_H/(12F)]^{1/2}, \quad \text{for } F \ll \pi\bar{a}f(h_c) \tag{27}$$

In the case of a drop of radius a approaching its homophase (flat oil–water interface), one has $\bar{a} = 2a$. In this case the buoyancy force $F \propto a^3$, see Eq. (23). Then, for spherical droplets one obtains

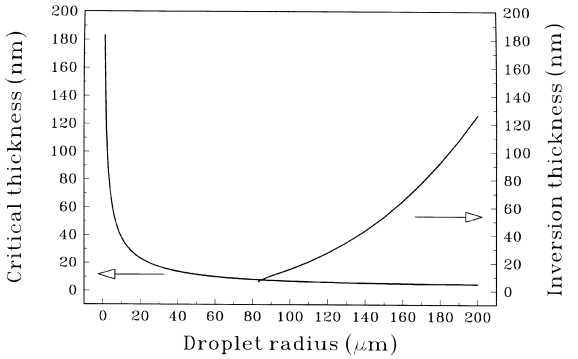

Fig. 5. Dependence of the critical and inversion thickness, h_c and h_i, on the droplet radius, a.

$h_c \propto 1/a$, i.e. the critical thickness markedly increases with the decrease of the droplet radius, see Fig. 5.

The curves in Fig. 5 are calculated for an emulsion system with aqueous phase solution of bovine serum albumin (BSA) with added 0.15 M NaCl. The salt suppresses the double layer repulsion; in addition, the BSA makes the oil–water interface tangentially immobile. The oil phase is soybean oil and the density difference is $\Delta\rho = 0.072$ g/cm^3. The interfacial tension is $\sigma = 15$ mN/m. Since, for the typical values of h_c the van der Waals interaction is affected by the electromagnetic retardation effect, we used an expression for A_H, proposed by Russel et al. [36]:

$$A_H = \frac{3h_P v}{4\pi} \frac{(n_o^2 - n_w^2)^2}{(n_o^2 + n_w^2)^{3/2}} \int_0^\infty \frac{(1+2\chi z)\exp(-2\chi z)}{(1+2z^2)^2} \, dz \tag{28}$$

Here, $h_P = 6.63 \times 10^{-34}$ J s is Planck's constant, $v = 3.0 \times 10^{15}$ Hz is the main electronic absorption frequency; $n_o = 1.418$ and $n_w = 1.333$ are the refractive indices of the oil and water phases; the dimensionless thickness χ is defined by the expression:

$$\chi = n_w (n_o^2 + n_w^2)^{1/2} \frac{2\pi v h}{c} \tag{29}$$

$c = 3.0 \times 10^{10}$ cm/s is the speed of light. For small thickness A_H, as given by Eqs. (28) and (29), is constant, whereas for large thickness h one obtains $A_H \propto h^{-1}$.

Fig. 5 shows the inversion (film formation)

thickness, h_i, and the critical thickness, h_c, as functions of the droplet radius, a, for the above specific system. To calculate h_i and h_c we combined Eqs. (16) and (24) with Eqs. (23), (25), (28) and (29). The calculation is made for an oil droplet approaching a horizontal oil–water interface under the action of the buoyancy force. One sees that h_i increases, whereas h_c decreases with the rise of the drop radius, a. The strong increase of h_c for the smallest drops is rather intriguing. It is interesting to note also that for droplet radii smaller than 83 μm, Eq. (16) has no solution for the system under consideration, i.e. the droplet surface remains always convex and there is no formation of a film. On the contrary, for droplet radii greater than 83 μm the critical thickness h_c is smaller than the inversion thickness h_i, i.e. the droplet surfaces will flatten in the zone of contact before the critical thickness is reached; thus a flat film can form, which eventually can rupture.

3.2.3. *Lifetime of oil drops attached below an oil–water interface*

As demonstrated in ref. [37], the theory of droplet lifetime, based on Eqs. (22) and (23), predicts that the curves of τ vs. a should exhibit a minimum in the region $a = 10$–100 μm. To check the predictions of the theory, experiments with soybean oil droplets in aqueous solution of BSA have been carried out [38]. The oil drops of various size have been released by means of a syringe in the aqueous solution; then the drops move upwards under the action of the buoyancy force and approach a horizontal oil–water interface. The lifetime, τ, of the drops beneath the interface has been measured as a function of the drop radius, a. The data are presented in Fig. 6. The continuous line in Fig. 6 is calculated by means of Eq. (22) along with Eqs. (19), (23)–(25), (28) and (29). For all drops, $h_{in} = 15$ μm was used in Eq. (22). Although this choice has no theoretical background (this is the thickness at which the drops become well visible), its arbitrariness does not affect substantially the results for τ. One sees in Fig. 6 that the theory agrees well with the experiment. The left branch of the curve corresponds to the Taylor regime (non-deformed droplets), whereas the right branch corresponds to the Reynolds regime (planar film between the droplets). The data of Dickinson et al.

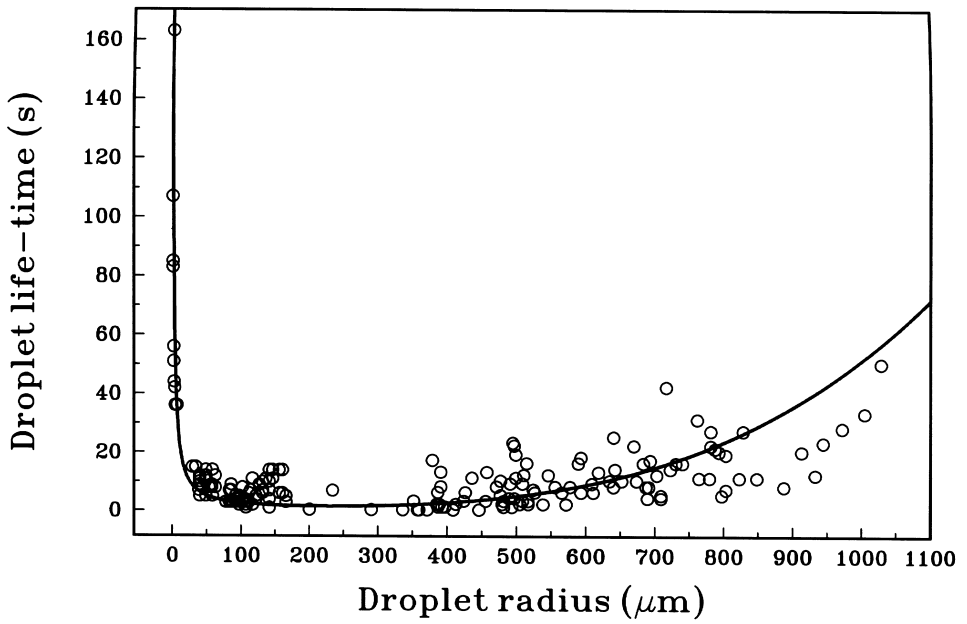

Fig. 6. Lifetime, τ, of oil-in-water drops approaching from below a water–oil interface as a function of the droplet radius [38]. The circles are experimental points for aqueous solutions of bovine serum albumin (BSA) with 0.15 M NaCl; the drops are of soybean oil. The theoretical curve is drawn by means of Eq. (22).

[39] for the same system correspond to the left branch (very small drops).

4. Drops with tangentially mobile surfaces: deformed drops with planar film

Below we consider another important hydrodynamic effect: the influence of the surfactant distribution and surface mobility on the coalescence rate. Two limiting cases can be distinguished. The first is related to the hydrodynamic interaction between two deformed emulsion drops [with film between them, Fig. 1(b)]; this case is considered in the present section. The second case corresponds to interaction between two non-deformed spherical drops, see Section 5 below. For tangentially immobile surfaces these two cases correspond to Reynolds and Taylor regimes respectively [see Eq. (18) and Eq. (14)]. The mathematical treatment in the former case is easier in so far as the problem can be reduced to the calculation of the flow between two parallel concentric disks, approaching each other.

4.1. Rate of approach of two deformed emulsion drops

The flux of the liquid expelled from the gap between two colliding emulsion drops has two main effects (see Fig. 7). (i) It carries the adsorbed surfactant molecules toward the periphery of the two film surfaces, thus triggering compensating bulk and surface diffusion fluxes. (ii) It exerts a viscous force on the film surfaces, which is opposed by the gradient of the interfacial tension (caused by the non-uniform surfactant distribution). Below we present the predictions of the theory for the velocity of thinning of emulsion films depending on whether the surfactant is soluble in the continuous or the drop phase.

4.1.1. Surfactant soluble in the continuous phase (System I)

When the surfactant is soluble in the continuous phase (we will call such a system "System I"), it turns out that the rate of film thinning V_I is governed mainly by the gradient of interfacial

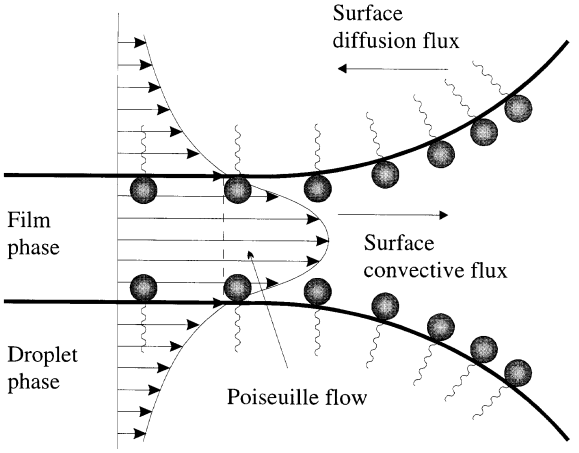

Fig. 7. Sketch of the velocity profile in the zone of contact between two deformed emulsion drops. The outflow of the liquid from the gap between the drops carries along the adsorbed surfactant molecules. The resulting gradients of the surfactant adsorption are opposed by the surface diffusion flux and surface elasticity, which tend to make the adsorption layer uniform.

tension (just as it is for foam films [27,30,40]), which is accounted for by the surface (Gibbs) elasticity, $E_G = -\Gamma(\partial\sigma/\partial\Gamma)$, where Γ denotes surfactant adsorption [27,30]:

$$\frac{V_I}{V_{Re}} \approx 1 + \frac{1}{\epsilon_f}, \quad \frac{1}{\epsilon_f} = \frac{6\eta_1 D_s}{hE_G} + \frac{3\eta_1 D}{\Gamma}\left(\frac{\partial c}{\partial \sigma}\right)_{eq} \qquad (30)$$

and the subscript "eq" denotes equilibrium values. Here, D and D_s are the bulk and surface diffusivities, c its bulk concentration, η_1 is the viscosity of liquid 1 (in which the surfactant is dissolved), and ϵ_f is the so-called foam parameter [27,30]. Note that the bulk and surface diffusion fluxes, which tend to restore the uniformity of the adsorption monolayers and thus to damp the surface tension gradients, accelerate the film thinning. [Since D_s in Eq. (30) is divided by the film thickness h, the effect of surface diffusion dominates the effect of bulk diffusion for small values of the film thickness.] On the other hand, the surface (Gibbs) elasticity, E_G (the Marangoni effect) decelerates the thinning. Eq. (30) predicts that System I behaves as a foam system: the rate of thinning is not affected by the circulation of liquid in the droplets.

4.1.2. Surfactant soluble in the drop phase (System II)

It was established theoretically [27,40] that when the surfactant is dissolved in the drop phase (System II in Fig. 8) it remains uniformly distributed on the surface during the film thinning and cannot create interfacial tension gradients. Hence, the system does not feel the surfactant and the rate of thinning, V_{II}, is the same as in the case of pure liquid phases:

$$\frac{V_{II}}{V_{Re}} \approx \frac{1}{\epsilon_e} \approx \frac{\eta_1 \delta}{\eta_2 h} \approx \left(\frac{108\pi\eta_1^3 R^4}{\rho_2 \eta_2 h^4 F} \right)^{1/3} \quad (31)$$

Here ϵ_e is called the emulsion parameter, δ is the thickness of the hydrodynamic boundary layer inside the drops, ρ_2 and η_2 are the density and viscosity of liquid 2, which does not contain dissolved surfactant. Eq. (31) was confirmed experimentally [41]. Qualitatively, the absence of Marangoni effect in this case can be attributed to the fact that the convection driven initial surface tension gradients are rapidly damped by the influx of surfactant from the drop interior (see refs. [27,30,40] for details).

4.1.3. Comparison of System I and System II

The only difference between the two systems in Fig. 8 is the exchange of the continuous and drop phases. Assume, for simplicity, that V_{Re} is the same for both systems. In addition, usually $\epsilon_f \approx 0.1$ and $\epsilon_e \approx 10^{-2}$–$10^{-3}$. Then, from Eqs. (30) and (31) one obtains [27,30,40]:

$$\frac{V_{II}}{V_I} \approx \frac{\epsilon_f}{\epsilon_e} \approx \frac{0.1}{10^{-2} \text{ to } 10^{-3}} \approx 10 \text{ to } 100$$

(deformed drops) (32)

Hence, the rate of film thinning in System I is much greater than that in System II. Therefore, the location of the surfactant has a dramatic effect on the thinning rate and thereby on the drop lifetime. Note also that the interfacial tension in both systems is the same. Hence, the mere phase inversion of an emulsion, from A/B to B/A, may change the emulsion lifetime by orders of magni-

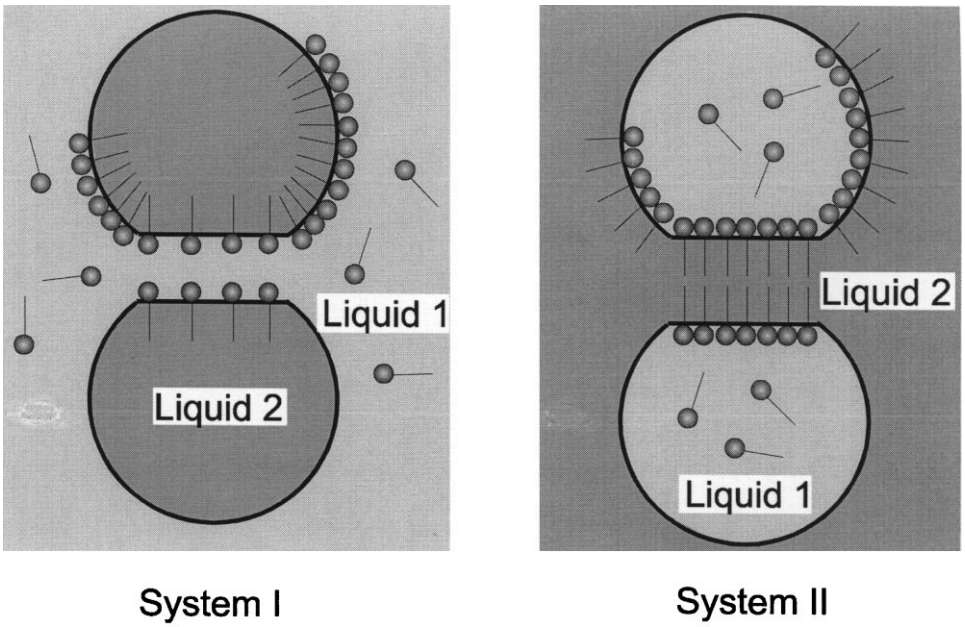

Fig. 8. Two complementary types of emulsion systems obtained by a mere exchange of the continuous phase with the disperse phase. The surfactant is assumed to be soluble in liquid 1.

tude. As demonstrated in Section 5 below, the situation with the interaction in Taylor regime (between spherical, non-deformed drops) is similar. These facts are closely related to the explanation of the Bancroft rule for the stability of emulsions (see Section 5.3 below) and the process of chemical demulsification, see ref. [37] for details.

4.2. Critical thickness of the gap between two deformed drops

When the drops are larger (say $a>50$ μm), an almost plane-parallel film of radius r is formed in the zone of their contact. As far as the rate of thinning V is concerned, it turns out (see ref. [42]) that such a film is equivalent to a plane-parallel film, provided that the film radius r is defined correctly. However, even small deviations from planarity (which are due to the non-uniform distribution of the pressure inside the gap) become important when solving the problem for the rupture of the film by growing fluctuational capillary waves. Indeed, the deviations from planarity can be greater than the amplitude of the fluctuation waves, and consequently they should be accounted for when estimating the critical thickness of film rupture, h_c. To take into account this effect one should base the theory on a more precise expression of the interfacial profile. Such an equation was reported in ref. [42]. The leading term in the equation of the interfacial shape, $H(\rho)$, is:

$$H(\rho)=h+\frac{\rho^2}{\bar{a}}-L\ln\left(1+\frac{\rho^2}{\bar{a}L}\right)-\frac{\rho^2}{2\bar{a}}\left(1+\frac{\rho^2}{\bar{a}L}\right)^{-1};$$

$$L\equiv\frac{F}{2\pi\bar{\sigma}} \tag{33}$$

where ρ is the radial coordinate and, as usual, h is the shortest distance between the surfaces of the two drops. We performed a fluctuation analysis (similar to the one outlined in Section 3.2.2) of the shape of the gap between two drops, Eq. (33), and obtained the following equation for the critical thickness, h_c:

$$\frac{2+d}{1+d}=\frac{h_c r^2}{8\bar{\sigma}[2\bar{\sigma}/\bar{a}-\Pi(h_c)]}\left(\frac{\partial\Pi}{\partial h}\right)_c^2 \tag{34}$$

Here

$$d\equiv\frac{h_s}{h(1+b)},\ h_s\equiv\frac{6\eta_1 D_s}{E_G},1.0$$

$$b\equiv\frac{3\eta_1 D}{E_G}\left(\frac{\partial c}{\partial\Gamma}\right)_{eq}=\frac{3\eta_1 D}{\Gamma}\left(\frac{\partial c}{\partial\sigma}\right)_{eq} \tag{35}$$

and D denotes the bulk diffusivity of the surfactant (dissolved in the continuous phase); as before, the subscript "eq" denotes equilibrium values. Eq. (34) shows that the disjoining pressure significantly influences the critical thickness. The influence of the surfactant enters the theory through the parameter d, the disjoining pressure Π, and the surface tension σ. Eq. (34) is valid for the case when the disjoining pressure is smaller than the capillary pressure $\Pi<P_c$, i.e. the film thins and ruptures before reaching its equilibrium thickness.

Numerical results obtained from Eq. (34) for an emulsion film stabilized by sodium dodecyl sulfate (SDS, below the critical micellization concentration) are shown in Figs. 9 and 10. The van der Waals and electrostatic interactions are taken into account in the calculation of the disjoining pressure Π. It is seen that for a given surfactant concentration and droplet radius, h_c increases with the rise of the film radius, r. The influence of the surfactant concentration on h_c is illustrated in Fig. 10. The radius of the film is taken to be $r=1$ μm and the calculations are performed for three

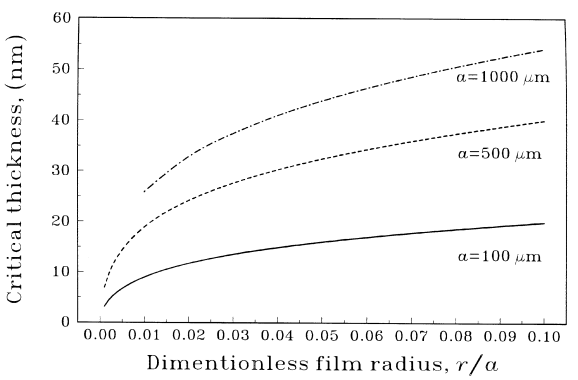

Fig. 9. Dependence of the critical thickness h_c on the dimensionless film radius r/a, calculated by means of Eq. (34); the values of the parameters correspond to 1 mM aqueous solution of sodium dodecyl sulfate (SDS); the drop (oil) phase is decane.

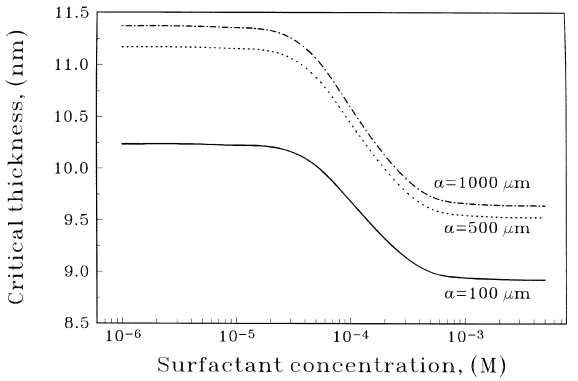

Fig. 10. Dependence of the critical thickness h_c on the surfactant (SDS) concentration for three values of the drop radius a, calculated by means of Eq. (34). The film radius is taken to be $r=10$ μm; the drop (oil) phase is decane.

different values of the droplet radius a. For all surfactant concentrations the increase of the droplet radius, a, leads to a larger critical thickness, h_c, and a lower stability of the corresponding film. On the other hand, the increase of surfactant concentration leads to smaller critical thickness and higher film stability for all values of a, see Fig. 10.

The latter effect was observed experimentally for free aniline films (in air) [30]. The experimental data for the dependence of h_c on the surfactant concentration (dodecanol plays the role of surfactant for the aniline films in ref. [30]) shows qualitatively the same behavior.

5. Drops with tangentially mobile surfaces: spherical non-deformed drops

It was shown long ago [27,30,40] that for deformed drops with a planar film the circulation of the liquid in the drop phase gives a negligible contribution to the energy dissipation when the surfactant is dissolved in the continuous phase. In other words, such drops behave like bubbles from a hydrodynamic viewpoint (this is a case of System I from Section 4.1.1). On the contrary, when the surfactant is in the drop phase it has no effect on the drainage rate and the system behaves as though there were no surfactant at all, i.e. as a system of pure liquids (System II in Section 4.1.2). Physical considerations suggest, and our preliminary calculations confirm, that the situation is similar with non-deformed spherical drops. Hence, to avoid unnecessary complications in what follows we will either neglect the circulation in the internal phase and treat the drops as bubbles (System I) or, when the surfactant is in the drop phase, we will treat the system as containing no surfactant at all (System II).

5.1. Drops of pure liquid (no surfactants)

When the surface of an emulsion droplet is mobile, it can transmit the motion of the outer fluid to the fluid within the droplet. This leads to a special circulation pattern of the fluid flow and affects the dissipation of energy in the system. The problem about the approach of two non-deformed (spherical) drops or bubbles in the absence of surfactants has been investigated by many authors [43–52]. A number of solutions, generalizing the Taylor Eq. (14), have been obtained. For example, the velocity of central approach of two spherical drops in pure liquid, V_p, is related to the driving force, F, by means of a Padé type expression derived by Davis et al. [51]:

$$V_p = V_{Ta}\frac{1+1.711\xi+0.461\xi^2}{1+0.402\xi},\quad \xi=\frac{\eta_{out}}{\eta_{in}}\sqrt{\frac{\bar{a}}{2h}};$$

$$V_{Ta}=\frac{2hF}{3\pi\eta\bar{a}^2} \tag{36}$$

where, as usual, h is the closest surface-to-surface distance between the two drops; η_{in} and η_{out} are the viscosities of the liquids inside and outside the droplets. In the limiting case of solid particles one has $\eta_{in}\to\infty$ and Eq. (36) reduces to the Taylor Eq. (14). Note that in the case of close approach of two drops ($\xi\gg1$) the velocity V_p is proportional to $\sqrt{h}$. This implies that the two drops can come into contact ($h=0$) in a finite period of time ($\tau<\infty$) under the action of a given force, F, because the integral in Eq. (22) is convergent for

$h_c=0$. In contrast, in the case of immobile interfaces ($\xi \ll 1$) one has $V_{Ta} \propto h$ and $\tau \to \infty$ for $h_c \to 0$.

Note that limiting cases of Eq. (36), valid for small and large values of ξ, were initially obtained in ref. [48]. Later, Davis et al. [51] found that all results in ref. [48] differ from his respective asymptotics by a factor of $\sqrt{2}$. The reason is the definition of the minimum gap width: it is h in ref. [48], whereas it is $2h$ in the paper of Davis et al. [51].

5.2. Drops (bubbles) with surfactants in the continuous phase

When the driving force F (say the Brownian or the buoyancy force) is small compared to the capillary pressure of the droplets, the deformation of the spherical droplets upon collision will only be a small perturbation in the zone of contact. Then the film thickness and the pressure within the gap can be presented as a sum of a non-perturbed part and a small perturbation. Solving the resulting linearized hydrodynamic problem for low interfacial viscosity, an analytical formula for the velocity of thinning, $V=-\mathrm{d}h/\mathrm{d}t$, can be derived [30]:

$$\frac{V}{\tilde{V}_{Ta}}=\frac{h_s}{2h}\left[\frac{d+1}{d}\ln(d+1)-1\right]^{-1},$$

$$\tilde{V}_{Ta}=\frac{2h}{3\pi\eta_1\bar{a}^2}(F-\pi\bar{a}f) \qquad (37)$$

where $\bar{a}$ is the "mean" droplet radius defined by Eq. (17); f is the interaction surface free energy per unit area; the dimensionless parameter d and the characteristic surface diffusion thickness h_s are defined by Eq. (35) above; $\tilde{V}_{Ta}$ is a generalized Taylor velocity of two non-deformed spherical solid particles approaching each other, in which the term $\pi\bar{a}f$ accounts for the force of intermolecular interaction between the two spherical particles; see Eq. (6) for the definition of f. It should also be noted that even for small deformations and small droplets the contribution of f can be significant. In the limiting case of very large interfacial elasticity E_G (tangentially immobile interface), the parameter d tends to zero and, in view of Eq. (35), one can check that Eq. (37) predicts $V \to \tilde{V}_{Ta}$, as should be expected.

The first Eq. (37) was in fact derived in ref. [42], but with V_{Ta}, i.e. without accounting for the interaction energy. It is noteworthy that its right-hand side, which accounts for the surface mobility, is the same, i.e. the surface interaction does not affect the hydrodynamic effects.

Below we give the generalizations of Eqs. (16) and (24) for the inversion thickness, h_i, and the critical thickness, h_c, for the case of tangentially mobile interfaces. We showed that the inversion thickness can be found as a solution of the following transcendental equation [32]:

$$h_i=\frac{F}{2\pi\bar{\sigma}}\phi(d)+\frac{\bar{a}}{2\bar{\sigma}}[h_i\Pi(h_i)-f(h_i)\phi(d)],$$

$$\phi(d)=\frac{d-\ln(d+1)}{(d+1)\ln(d+1)-d} \qquad (38)$$

The effect of the interfacial mobility is accounted for by the function $\phi(d)$. For large interfacial elasticity, E_G, one has $d \ll 1$, see Eq. (35); then $\phi(d)=1$ and Eq. (38) reduces to the result for tangentially immobile interface, Eq. (16). In the other limit, of small interfacial elasticity, the value of ϕ decreases with the decrease of E_G. Then Eq. (38) shows that the higher the interfacial mobility (the smaller ϕ), the lower the inversion thickness h_i. The attractive surface forces lead to smaller inversion thickness. For large negative (attractive) Π, Eq. (38) has no solution for h_i, i.e. the drop surface remains convex during the entire dynamic stage of the drop–drop collision (at the equilibrium state, if any, flattening in the zone of contact could eventually appear).

In order to investigate the film stability one can introduce, in the same way as described in Section 3.2.2 above, small oscillatory perturbations of the droplet shape and pressure distribution. The aim is to generalize Eq. (24) for the critical thickness, h_c, for two non-deformed spherical droplets by accounting for the effect of Marangoni. Numerical solution of this problem is reported in ref. [34]. It was proven that the long waves represent the most unstable modes. This finding allows one to derive an analytical equation for determin-

ing the critical thickness h_c [32]:

$$[F-\bar{a}\pi f(h_c)]\psi(d)=\frac{\pi\bar{a}^2h_c^3}{32\bar{\sigma}}\left[\left(\frac{\partial\Pi}{\partial h}\right)_c^2-\frac{8\bar{\sigma}}{\bar{a}}\left(\frac{\partial^2\Pi}{\partial h^2}\right)_c\right]$$

where

$$\psi(d)=\frac{(d+2)d^2}{4(d+1)^2[(d+1)\ln(d+1)-d]}$$

The comparison of Eq. (39) with Eq. (24) shows that the function $\psi(d)$ accounts for the effect of the surface mobility. Indeed, for large interfacial elasticity one has $d\to 0$; then $\psi\to 1$ and Eq. (39) reduces to Eq. (24). In the other limit, small interfacial elasticity, one has $d\gg 1$ and in such a case $\psi\propto 1/\ln d$, i.e. ψ decreases with the increase of d, that is with the decrease of E_G. The decreasing of $\psi(d)$ (increasing of surface mobility) in Eq. (39) leads to a decrease of the force and in such a way to smaller critical thickness.

5.3. Interpretation of the Bancroft rule

The Bancroft rule [53] for the stability of emulsions states that "in order to have a stable emulsion the surfactant must be soluble in the continuous phase". Davies and Rideal [54] assumed that both types of emulsions are formed during the homogenization process, but only the one with the lower coalescence rate survives. We have already applied this concept to justify theoretically an "extended" Bancroft rule for relatively large deformed drops (with a planar film between them) by accounting for the interdroplet interaction [37]. Our goal is now to do the same for spherical non-deformed drops, which is usually the case in the range of micron and submicron drop size.

Let us consider an oil–water system in which the surfactant is soluble only in the aqueous phase. In the highly dynamic process of emulsion formation by stirring (homogenization), both oil-in-water emulsion (System I) and water-in-oil emulsion (System II) appear. The coalescence rates for the two emulsions will be (approximately) proportional to the respective velocities of film thinning, V_I and V_{II} [37,55]:

$$\frac{\text{Rate II}}{\text{Rate I}}\approx\frac{V_{II}}{V_I} \tag{40}$$

Let us first consider the case of System II (surfactant inside the drops) in which case the two drops approach each other like drops from pure liquid phases (see Section 5.1). Therefore, for the velocity of approach of two such aqueous droplets, one can use the following approximate expression:

$$V_{II}/\tilde{V}_{Ta}^{(II)}\approx 0.811\,\frac{\eta_2}{\eta_1}\sqrt{\frac{\bar{a}}{h}} \tag{41}$$

Eq. (41) follows directly from Eq. (36) for $\xi\gg 1$. As before, we denote by η_1 the viscosity of the liquid phase in which the surfactant is soluble, and by η_2 the viscosity of the phase which does not contain dissolved surfactant.

The velocity of droplet approach in System I, V_I, can be expressed by means of Eq. (37). Note that the Taylor velocities for System I and System II, $\tilde{V}_{Ta}^{(I)}$ and $\tilde{V}_{Ta}^{(II)}$, are different because of differences in viscosity and droplet–droplet interaction, see Eq. (37). Then, combining Eqs. (37), (40) and (41) we arrive at the following criterion for formation of emulsion of type I or II:

$$\frac{\text{Rate II}}{\text{Rate I}}\approx\frac{V_{II}}{V_I}=0.811\sqrt{\frac{\bar{a}}{h}}\frac{2h}{h_s}\times\left[\frac{d+1}{d}\ln(d+1)-1\right]\frac{(F-\pi\bar{a}f)_{II}}{(F-\pi\bar{a}f)_I} \tag{42}$$

In the case of sufficiently large surface (Gibbs) elasticity, $E_G\gg 1$, one has $d\ll 1$, and in view of Eq. (35) one can expand the logarithm in Eq. (42) to obtain:

$$\frac{\text{Rate II}}{\text{Rate I}}\approx\frac{V_{II}}{V_I}\approx 0.811\sqrt{\frac{\bar{a}}{h_c}}\frac{1-d/3+O(d^2)}{1+b}\frac{(F-\pi\bar{a}f)_{II}}{(F-\pi\bar{a}f)_I} \tag{43}$$

Here we have used the fact that at the moment of coalescence h should be equal to the critical thick-

ness of drop coalescence, $h=h_c$. For typical emulsion systems ($\bar{a}\gg h_c$), Eq. (43) yields Rate II/Rate I$\gg$1; therefore System I (with surfactant dissolved in the continuous phase) will survive. This is a prediction which essentially coincides with the Bancroft rule. The following more specific conclusions can also be drawn from Eqs. (42) and (43).

(1) The effect of droplet size $\bar{a}$ can be deduced from Eq. (43). For larger droplets (larger $\bar{a}$) the critical thickness h_c is smaller (see Fig. 5) and the difference between the coalescence rates in Systems I and II becomes larger. On the other hand, the difference between Rate I and Rate II decreases with the reduction of the droplet size $\bar{a}$, which is accompanied by an increase of the critical thickness h_c (see Fig. 5). Note that this effect of $\bar{a}$ cannot be derived from the criterion for essentially deformed drops, see Eq. (27) in ref. [37].

(2) The interactions of intermolecular origin, accounted for by f, can be rather different for Systems I and II because of the different types of surface forces operative in water and oil films. However, for both systems it is true that the external and intermolecular forces are counterbalanced at equilibrium, i.e. $F=\pi\bar{a}f$. If System II reaches equilibrium faster than System I (for example, this can happen when long-range electrostatic or steric repulsive forces are operative between the droplets in System II), then the term $(F=\pi\bar{a}f)_{II}$ in Eq. (43) tends to zero and one can obtain Rate II/Rate I$\ll$1, i.e. System II will survive. This is exactly the opposite to the prediction of the Bancroft rule, which is not valid in this case. Such deviations from the Bancroft rule have been experimentally observed, see ref. [12].

(3) The effect of the bulk viscosity is not explicitly present in Eq. (43), although there could be some weak implicit dependence through the parameters d and b, see Eq. (35). This conclusion agrees with the experimental observations, which show a very weak dependence of the volume fraction of phase inversion on the viscosity of the continuous phase (see ref. [54], p. 381).

(4) The increase of the bulk and surface diffusivities, D and D_s, which tend to damp the surface tension gradients, leads to an increase of the parameters b and d, which decreases the difference between Rate I and Rate II, see Eqs. (35) and (43).

(5) On the contrary, the increase of the surface (Gibbs) elasticity, E_G, leads to a decrease of d and thus favors the survival of System I, see Eq. (43). In the limit of tangentially immobile interfaces ($E_G\to\infty$) one has $d=0$ and $b=0$ and the criterion (43) further simplifies:

$$\frac{\text{Rate II}}{\text{Rate I}}\approx\frac{V_{II}}{V_I}\approx 0.811\sqrt{\frac{\bar{a}}{h_c}}\frac{(F-\pi\bar{a}f)_{II}}{(F-\pi\bar{a}f)_I}\quad(E_G\to\infty) \tag{44}$$

(6) The effect of surface viscosity, η_s, is neglected when deriving Eqs. (43) and (44). Based on the hydrodynamic equations one can estimate that the effect of the surface viscosity, η_s, on V_I and V_{II} is negligible when:

$$\frac{\eta\bar{a}^2}{\eta_s h}\gg 1 \tag{45}$$

where η stands for the bulk viscosity, which is assumed to be of the same order of magnitude for the liquids inside and outside the drops. If, for a certain system, η_s is large and the criterion, Eq. (45), is not satisfied, then one can expect that the surface viscosity will suppress the interfacial mobility for both Systems I and II. Then the difference between Rate I and Rate II will be determined mostly by the intermolecular interaction energy, f. Note that typically f facilitates the flocculation in water-in-oil emulsions.

It seems pertinent to make a few remarks about the validity of the present justification of the extended Bancroft rule as well as of that reported previously in ref. [37], referring to the case of large drops (with planar films between them). Although we reached somewhat more general conclusions than the original Bancroft rule [e.g. the possibility for inversion of the emulsion stability due to the interaction energy, see point (2) above], we neither claim that the Bancroft rule or our extension of it have general validity, nor that we have given a general explanation of the emulsion stability. The latter is such a complex phenomenon, and there are so many different systems with different dominant factors involved, that, according to us, any attempt at a general explanation (or theory) is hopeless. Our treatment is theoretical and, as for

every theory, it has limitations inherent to the model used and therefore is valid only under specific conditions. It should not be applied to systems where these conditions are not fulfilled, although it may happen that sometimes it works even then, but this is most probably a fortuitous coincidence. The reader may find in the quoted original papers detailed formulation of the models and assumptions used. The main ones are:

- planar films or spherical drops (no dimple);
- no forces (like the curvature effects studied by Kabalnov and coworkers [56,57]) opposing the expansion of the hole formed in the film after the two drops have "touched" each other;
- the surfactant transfer onto the surface is diffusion controlled;
- the surfactant concentration is below the CMC (no effects either of the demicellization kinetics or stratification or other structural effects unless they are incorporated in the disjoining pressure);
- no effect of the interfacial viscosity is accounted for;
- only small perturbations in the surfactant distribution, which are due to the flow, are considered; with strongly non-equilibrium distribution we found that new effects come into play, which may totally change the contribution of the effects and inverse the stability ratio.

6. Concluding remarks

One important conclusion is that the occurrence of flocculation in an emulsion is significantly affected by the appearance of deformation (flattening, film) in the zone of contact of two interacting droplets. The appearance of such a deformation has the following consequences.

(i) It enhances the importance of the surface forces of intermolecular origin and gives rise to contributions from the interfacial dilatation and the bending energy, reviewed in Section 2 above.

(ii) The flattening increases the viscous dissipation in the gap between two colliding drops and thus prolongs the lifetime of the doublet of two such drops, see Eq. (22) and Fig. 6. This effect is related to points (iii) and (iv) below.

(iii) The velocity of approach is different for two deformed and non-deformed drops, cf. Eqs. (30) and (31) with Eqs. (37) and (41).

(iv) The critical thickness of the gap between two droplets also depends on whether the drops are deformed or non-deformed, cf. Eq. (34) and Fig. 5 with Eqs. (24) and (39) and Figs. 9 and 10.

The factors which facilitate the flattening in the zone of contact between two emulsion drops are the following.

(i) The increase of droplet size, see Eq. (22) and Fig. 6.

(ii) The decrease of the interfacial tension, σ, see Eqs. (2) and (19).

(iii) The bending energy for water-in-oil emulsions, see Eq. (3).

(iv) The increase of the droplet–droplet attraction and suppression of the droplet–droplet repulsion, see Eq. (12) and Figs. 2 and 3.

(v) The decrease of the tangential mobility of the interfaces, see the discussion after Eq. (38).

(vi) The high droplet volume fraction forces the emulsion drops to deform because of the restricted volume; for high drop volume fractions emulsions of foam-like structure are formed.

(vii) The larger the external force, F, exerted on the droplets, the larger the deformation upon collision, see Eq. (19); this effect could be significant in the early stages of emulsion formation, when as a rule a turbulent regime is present and strong drag forces are exerted on the droplets.

Finally, let us try to summarize the major effects due to the presence and transport of surfactant in the emulsion systems.

(i) The surfactant strongly affects the interfacial tension, σ, and bending moment, B_0, see Eqs. (2), (3) and (19).

(ii) The presence of surfactant adsorption monolayers and surfactant micelles in the films influences all kinds of DLVO and non-DLVO surface forces considered in Section 2.3 above.

(iii) The rheological and dynamic properties of the surfactant adsorption monolayers (Gibbs elasticity, E_G, surface diffusivity, D_s, surface viscosity, η_s, and adsorption relaxation time) determine the stability of emulsions under

dynamic conditions, see e.g. Eqs. (30), (32), (34), (35), (38), (39), (42) and (43).

(iv) The solubility of the surfactant in one of the two phases can determine whether the oil-in-water or water-in-oil emulsion will be formed, see Section 5.3.

(v) In the case of emulsions from non-pre-equilibrated oil and water phases, the process of transfer of surfactant from the continuous phase toward the droplets (or vice versa) is found to have a stabilizing effect, see refs. [58–61]. On the contrary, the process of surfactant transfer from one emulsion drop to another is found to have a destabilizing action [62–64].

Acknowledgments

This study was supported in part by Kraft General Foods, Inc., and in part by the Bulgarian National Science Fund.

References

[1] K.D. Danov, N.D. Denkov, D.N. Petsev, R. Borwankar, Langmuir 9 (1993) 1731.
[2] D.N. Petsev, N.D. Denkov, P.A. Kralchevsky, J. Colloid Interface Sci. 176 (1995) 201.
[3] M.P. Aronson, H. Princen, Nature 296 (1980) 370.
[4] M.P. Aronson, H. Princen, Colloids Surf. 4 (1982) 173.
[5] J.A.M.H. Hofman, H.N. Stein, J. Colloid Interface Sci. 147 (1991) 508.
[6] N.D. Denkov, P.A. Kralchevsky, I.B. Ivanov, C.S. Vassilieff, J. Colloid Interface Sci. 143 (1991) 157.
[7] N.D. Denkov, D.N. Petsev, K.D. Danov, J. Colloid Interface Sci. 176 (1995) 189.
[8] K.D. Danov, D.N. Petsev, N.D. Denkov, R. Borwankar, J. Chem. Phys. 99 (1993) 7179.
[9] N.D. Denkov, D.N. Petsev, K.D. Danov, Phys. Rev. Lett. 71 (1993) 3327.
[10] P.A. Kralchevsky, T.D. Gurkov, K. Nagayama, J. Colloid Interface Sci. 180 (1996) 619.
[11] G.J.M. Koper, W.F.C. Sager, J. Smeets, D. Bedeaux, J. Phys. Chem. 99 (1995) 13291.
[12] B.P. Binks, Langmuir 9 (1993) 25.
[13] B.P. Binks, Ann. Rep. Roy. Soc. Chem. C 92 (1996) 97.
[14] E.J.W. Verwey, J.Th.G. Overbeek, Theory of Stability of Lyophobic Colloids, Elsevier, Amsterdam, 1948.
[15] B.V. Derjaguin, N.V. Churaev, V.M. Muller, Surface Forces, Plenum Press, New York, 1987.
[16] J.N. Israelachvili, Intermolecular and Surface Forces, Academic Press, London, 2nd edn., 1991.
[17] P.A. Kralchevsky, K.D. Danov, N.D. Denkov, in: K.S. Birdi (Ed.), Handbook of Surface and Colloid Chemistry, CRC Press, New York, 1997, p. 333.
[18] P. Attard, D.J. Mitchell, B.W. Ninham, J. Chem. Phys. 89 (1988) 4358.
[19] J.K. Angarska, K.D. Tachev, P.A. Kralchevsky, A. Mehreteab, G. Broze, J. Colloid Interface Sci. 200 (1998) 31.
[20] V.N. Paunov, R.I. Dimova, P.A. Kralchevsky, G. Broze, A. Mehreteab, J. Colloid Interface Sci. 182 (1996) 239.
[21] J.N. Israelachvili, H. Wennerström, J. Phys. Chem. 96 (1992) 520.
[22] G.A.E. Aniansson, J. Phys. Chem. 82 (1978) 2805.
[23] D.T. Wasan, A.D. Nikolov, P.A. Kralchevsky, I.B. Ivanov, Colloids Surf. 67 (1992) 139.
[24] P.A. Kralchevsky, N.D. Denkov, Chem. Phys. Lett. 240 (1995) 385.
[25] K.G. Marinova, T.D. Gurkov, G.B. Bantchev, P.A. Kralchevsky, in: Proc. 2nd World Congress on Emulsions, Bordeaux, 1997, Paper No. 2-3-151.
[26] K.G. Marinova, T.D. Gurkov, T.D. Dimitrova, R.G. Alargova, D. Smith, Langmuir 14 (1998) 2019.
[27] I.B. Ivanov, D.S. Dimitrov, in: I.B. Ivanov (Ed.), Thin Liquid Films, Marcel Dekker, New York, 1988, p. 379.
[28] P. Taylor, Proc. Roy. Soc. (London) A108 (1924) 11.
[29] I.B. Ivanov, B.P. Radoev, T. Traykov, D. Dimitrov, E. Manev, Chr. Vassilieff, Hydrodynamics of foam and emulsion films, in: E. Wolfram (Ed.), Proc. Int. Conf. on Colloid and Surface Science, vol. 1, Akademia Kiado, Budapest, 1975, p. 583.
[30] I.B. Ivanov, Pure Appl. Chem. 52 (1980) 1241.
[31] P.A. Kralchevsky, K.D. Danov, I.B. Ivanov, Thin liquid film physics, in: R.K. Prud'homme (Ed.), Foams: Theory, Measurements and Applications, Marcel Dekker, New York, 1995, p. 86.
[32] K.D. Danov, I.B. Ivanov, in: Proc. 2nd World Congress on Emulsion, Bordeaux, 1997, Paper No. 2-3-154.
[33] O. Reynolds, Philos. Trans. Roy. Soc. (London) A177 (1886) 157.
[34] K.D. Danov, P.A. Kralchevsky, I.B. Ivanov, in: H. Zoller, G. Broze (Eds.), Handbook of Detergents, vol. 2, Properties, Marcel Dekker, New York, 1998, chapter 9, in press.
[35] I.B. Ivanov, B.P. Radoev, E.D. Manev, A.D. Scheludko, Trans. Faraday Soc. 66 (1970) 1262.
[36] W.B. Russel, D.A. Saville, W.R. Schowalter, Colloidal Dispersions, Cambridge University Press, 1989, p. 155.
[37] I.B. Ivanov, P.A. Kralchevsky, Colloids Surf. 128 (1997) 155.
[38] E.S. Basheva, I.B. Ivanov, T.D. Gurkov, G. Banchev, Langmuir (1998), to be submitted.
[39] E. Dickinson, B.S. Murray, G. Stainsby, J. Chem. Soc., Faraday Trans. 84 (1988) 871.
[40] T.T. Traykov, I.B. Ivanov, Int. J. Multiphase Flow 3 (1977) 471.
[41] T.T. Traykov, E.D. Manev, I.B. Ivanov, Int. J. Multiphase Flow 3 (1977) 485.

[42] I.B. Ivanov, D.S. Dimitrov, P. Somasundaran, R.K. Jain, Chem. Eng. Sci. 40 (1985) 137.
[43] E. Rushton, G.A. Davies, Appl. Sci. Res. 28 (1973) 37.
[44] S. Haber, G. Hetsroni, A. Solan, Int. J. Multiphase Flow 1 (1973) 57.
[45] L.D. Reed, F.A. Morrison, Int. J. Multiphase Flow 1 (1974) 573.
[46] G. Hetsroni, S. Haber, Int. J. Multiphase Flow 4 (1978) 1.
[47] F.A. Morrison, L.D. Reed, Int. J. Multiphase Flow 4 (1978) 433.
[48] V.N. Beshkov, B.P. Radoev, I.B. Ivanov, Int. J. Multiphase Flow 4 (1978) 563.
[49] D.J. Jeffrey, Y. Onishi, J. Fluid Mech. 139 (1984) 261.
[50] Y.O. Fuentes, S. Kim, D.J. Jeffrey, Phys. Fluids 31 (1988) 2445.
[51] R.H. Davis, J.A. Schonberg, J.M. Rallison, Phys. Fluids A1 (1989) 77.
[52] X. Zhang, R.H. Davis, J. Fluid Mech. 230 (1991) 479.
[53] W.D. Bancroft, J. Phys. Chem. 17 (1913) 514.
[54] J.T. Davies, E.K. Rideal, Interfacial Phenomena, Academic Press, New York, 1963.
[55] I.B. Ivanov, Lectures at INTEVEP, Petroleos de Venezuela, Caracas, June 1995.
[56] A. Kabalnov, H. Wennerström, Langmuir 12 (1996) 276.
[57] A. Kabalnov, J. Weers, Langmuir 12 (1996) 1931.
[58] O.D. Velev, T.D. Gurkov, R.P. Borwankar, J. Colloid Interface Sci. 159 (1993) 497.
[59] K.D. Danov, T.D. Gurkov, T.D. Dimitrova, D. Smith, J. Colloid Interface Sci. 188 (1997) 313.
[60] O.D. Velev, T.D. Gurkov, I.B. Ivanov, R.P. Borwankar, Phys. Rev. Lett. 75 (1995) 264.
[61] T.D. Gurkov, K.D. Danov, O.D. Velev, I.B. Ivanov, R.P. Borwankar, in: Proc. 2nd World Congress on Emulsion, Bordeaux, 1997, Paper No. 2-3-155.
[62] K.D. Danov, I.B. Ivanov, Z. Zapryanov, E. Nakache, S. Raharimalala, Marginal stability of emulsion thin film, in: M. Velarde (Ed.), Proc. Conf. on Synergetics, Order and Chaos, World Scientific, Singapore, 1988, p. 178.
[63] I.B. Ivanov, S.K. Chakarova, B.I. Dimitrova, Colloids Surf. 22 (1987) 311.
[64] B.I. Dimitrova, I.B. Ivanov, E. Nakache, J. Dispers. Sci. Technol. 9 (1988) 321.